Technical Report

UCAM-CL-TR-539
ISSN 1476-2986

Number 539

UNIVERSITY OF CAMBRIDGE
Computer Laboratory

Towards a ternary interpolating subdivision scheme for the triangular mesh

N.A. Dodgson, M.A. Sabin, L. Barthe, M.F. Hassan

July 2002

15 JJ Thomson Avenue
Cambridge CB3 0FD
United Kingdom
phone +44 1223 763500

http://www.cl.cam.ac.uk/

Technical reports published by the University of Cambridge
Computer Laboratory are freely available via the Internet:

http://www.cl.cam.ac.uk/TechReports/

Series editor: Markus Kuhn

ISSN 1476-2986

Towards a ternary interpolating subdivision scheme for the triangular mesh

N. A. Dodgson*, M. A. Sabin†, L. Barthe, M. F. Hassan
University of Cambridge Computer Laboratory,
15 J J Thomson Avenue, Cambridge, UK, CB3 0FD

July 10, 2002

Abstract

We derive a ternary interpolating subdivision scheme which works on the regular triangular mesh. It has quadratic precision and fulfils the standard necessary conditions for $C2$ continuity. Further analysis is required to determine its actual continuity class and to define its behaviour around extraordinary points.

1 Introduction

Building on our discovery of a family of $C2$ ternary interpolating univariate subdivision schemes [5] we investigate the possibility of there being useful ternary interpolating subdivision schemes on the triangular mesh. The hope is that we will find a $C2$ interpolating scheme for triangular meshes. Derivation of the ternary scheme mirrors that of the binary butterfly scheme [2] from the binary univariate interpolating scheme.

We first present the univariate interpolating subdivision schemes in both binary and ternary cases. We then demonstrate the derivation of the binary butterfly scheme, which has a single free parameter. We perform the same derivation for the ternary interpolating scheme, which has three free parameters.

It remains to perform analysis to find the continuity class of the derived scheme, to determine the best values for the three free parameters, and to define the scheme's behaviour around extraordinary points.

2 Univariate interpolating subdivision schemes

Binary and ternary interpolating subdivision schemes have been derived by Dyn *et al* [4] and Hassan *et al* [5] respectively. The non-trivial stencils of these schemes can be seen in Figure 1. Their masks are:

$$[b\ 0\ a\ 1\ a\ 0\ b] \qquad \text{binary} \tag{1}$$

$$[d\ c\ 0\ b\ a\ 1\ a\ b\ 0\ c\ d] \qquad \text{ternary} \tag{2}$$

*correspondence should be sent by e-mail to: nad@cl.cam.ac.uk
†also at Numerical Geometry Ltd.

Figure 1: The non-trivial stencils of the binary (left) and ternary (right) univariate subdivision schemes.

where, in the binary case:

$$\begin{aligned} a &= \tfrac{1}{2} + w & (3)\\ b &= -w & (4) \end{aligned}$$

with the scheme being $C1$ for $0 < w < \frac{1}{8}$ and the commonly-used scheme being the case when $w = \frac{1}{16}$. The z-transform of the scheme can be divided by the binary box-spline mask, $(1+z)$, twice for general w and four times for the special case of $w = \frac{1}{16}$. In the latter case the z-transform is:

$$\tfrac{1}{16}(-1 + 9z^2 + 16z^3 + 9z^4 - z^6) = \tfrac{1}{16}(1 + z)^4(-1 + 4z - z^2) \qquad (5)$$

It is not clear what behaviour is indicated by the ability to divide a scheme by the box-spline k times. It does show that the maximum possible continuity of the limit curve is $C(k-1)$ because the proof that a scheme has continuity $C(k-1)$ requires analysis of a Laurent polynomial which can be multiplied by $(1+z)^k$ to produce the z-transform of the scheme [1, 2], thus this Laurent polynomial must exist for the proof to proceed. While this gives a maximum, the actual continuity may be of a lower order. The triangular mesh schemes, which are derived later, also have the property that they can be divided by box-splines.

In the ternary case:

$$\begin{aligned} a &= \tfrac{1}{18}(13 + 9\mu) & (6)\\ b &= \tfrac{1}{18}(7 - 9\mu) & (7)\\ c &= \tfrac{1}{18}(-1 - 3\mu) & (8)\\ d &= \tfrac{1}{18}(-1 + 3\mu) & (9) \end{aligned}$$

with the scheme being $C2$ for $\frac{1}{15} < \mu < \frac{1}{9}$. The z-transform of this scheme can be divided by the ternary box-spline mask $(1 + z + z^2)$ three times to get:

$$\tfrac{1}{18}(1+z+z^2)^3((-1+3\mu)+(2-12\mu)z+(18\mu)z^2+(2-12\mu)z^3+(-1+3\mu)z^4). \quad (10)$$

If $\mu = \frac{1}{27}$ then an extra factor of $(1 + z + z^2)$ can be extracted, but this value of μ lies outside the range of values for which the scheme is $C2$. Again, it is not clear whether any useful conclusions can be drawn from the number of times that we can divide through by the box-spline mask.

3 Bivariate binary subdivision

The *butterfly* subdivision scheme [3] is an extension of the binary univariate subdivision scheme to the case of the triangular mesh. Figure 2 shows the stencil used to generate a new vertex's value in the regular case. It is necessary

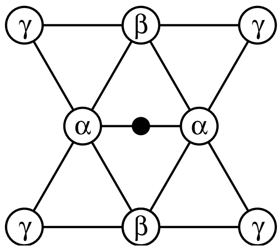

Figure 2: The non-trivial stencil of the butterfly scheme in the regular case.

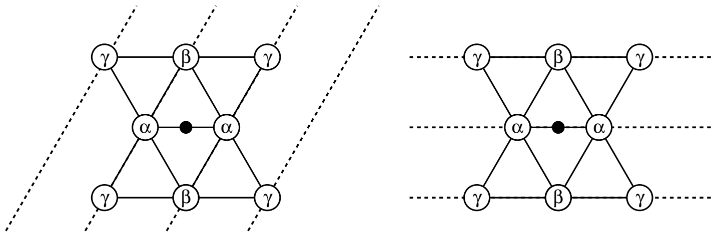

Figure 3: The mechanism for deriving the butterfly scheme from the binary univariate interpolating scheme. In each diagram assume that the control points have a constant value along each dotted line. In the left hand case, the interpolated point must match that which would be interpolated by the univariate scheme. In the right hand case the interpolated point must match the constant value.

to derive values for α, β, and γ. Dyn [2] does this by considering the cases shown in Figure 3. In these, each of the dotted lines indicates a set of vertices with the same value. The new vertex's value must be that which would be generated by the univariate scheme for the left-hand case in Figure 3, and must be the appropriate constant for the right-hand case. The left-hand case leads to the two equations:

$$a = \beta + \alpha + \gamma \tag{11}$$
$$b = \gamma \tag{12}$$

where a and b are defined in Equations 3 and 4. The right-hand case leads to the two equations:

$$0 = \beta + 2\gamma \tag{13}$$
$$1 = 2\alpha \tag{14}$$

Combined with the standard condition that all values in the stencil must sum to one ($2\alpha + 2\beta + 4\gamma = 1$), we get:

$$\alpha = \frac{1}{2} \tag{15}$$
$$\beta = 2w \tag{16}$$
$$\gamma = -w \tag{17}$$

$$\begin{bmatrix} & & 0 & \gamma & \gamma & 0 & \\ & \gamma & 0 & \beta & 0 & \gamma & \\ \gamma & \beta & \alpha & \alpha & \beta & \gamma & \\ 0 & 0 & \alpha & 1 & \alpha & 0 & 0 \\ & \gamma & \beta & \alpha & \alpha & \beta & \gamma \\ & & \gamma & 0 & \beta & 0 & \gamma \\ & & & 0 & \gamma & \gamma & 0 \end{bmatrix} = \begin{bmatrix} 1 & 1 & \\ 1 & 2 & 1 \\ & 1 & 1 \end{bmatrix} * \begin{bmatrix} & 0 & \gamma & 0 & \\ \gamma & \pi & \pi & \gamma & \\ 0 & \pi & \sigma & \pi & 0 \\ & \gamma & \pi & \pi & \gamma \\ & & 0 & \gamma & 0 \end{bmatrix}$$

Figure 4: The mask of the butterfly scheme (left) can be decomposed into a discrete convolution of the three-direction box-spline mask (centre) with the mask at right.

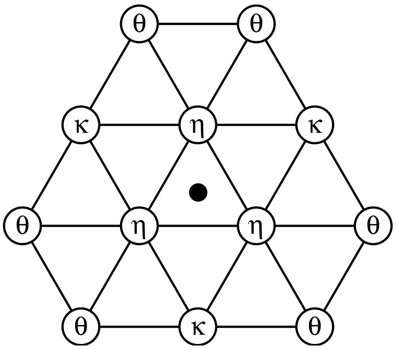

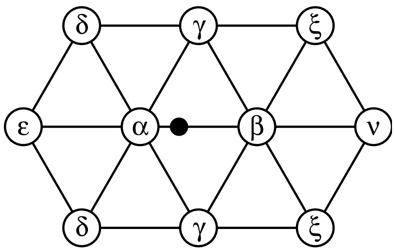

Figure 5: The non-trivial stencils of the ternary interpolating scheme in the regular case.

For the special case of $w = \frac{1}{16}$, we get the scheme which is generally implemented. Dyn [2] states that the butterfly scheme is $C1$ on a regular grid for $0 < w < w^*$. While we know that $w^* > \frac{1}{16}$, the maximum value of w^* is not known.

The butterfly scheme's mask can be divided by the three-direction box-spline mask to give a smaller mask, as shown in Figure 4. Here, we can calculate that:

$$\gamma = -w \tag{18}$$
$$\pi = 2w \tag{19}$$
$$\sigma = \tfrac{1}{2} - 6w \tag{20}$$

This decomposition is used in the analysis of the continuity of the butterfly scheme [1]. It is not certain what other conclusions can be drawn from the fact that the scheme can be decomposed into convolution of a smaller mask with the three-direction box-spline.

4 Bivariate ternary subdivision: derivation

Ternary interpolating subdivision on a triangular mesh has two non-trivial stencils on the regular grid. Figure 5 shows these stencils with ten unknowns. These are the maximum size that the stencils can be while keeping the mask within the 2-ring on the original triangular mesh. It may be that some of the unknowns could be set equal to zero.

Applying the condition that each stencil must sum to one gives:

$$6\theta + 3\kappa + 3\eta = 1 \tag{21}$$
$$2\delta + 2\gamma + 2\xi + \epsilon + \alpha + \beta + \nu = 1 \tag{22}$$

The "constant line" conditions provide equations for the ten unknowns in terms of the four known univariate parameters a, b, c, and d (Equations 6–9). For the left-hand stencil in Figure 5, we get (from top row to bottom row in the Figure):

$$d = 2\theta \tag{23}$$
$$b = \eta + 2\kappa \tag{24}$$
$$a = 2\eta + 2\theta \tag{25}$$
$$c = \kappa + 2\theta \tag{26}$$

For the right-hand stencil in Figure 5, we get (for the top and middle rows in the Figure, the bottom row being equivalent to the top):

$$0 = \delta + \gamma + \xi \tag{27}$$
$$1 = \epsilon + \alpha + \beta + \nu \tag{28}$$

and (for the left diagonal through to the right diagonal):

$$c = \delta + \epsilon \tag{29}$$
$$a = \gamma + \alpha + \delta \tag{30}$$
$$b = \xi + \beta + \gamma \tag{31}$$
$$d = \nu + \xi \tag{32}$$

This set of equations can be solved to give the ten unknowns in terms of three parameters: μ from the original Equations 6–9, along with ϵ and ν, two of the unknowns:

$$\theta = \tfrac{1}{36}(-1 + 3\mu) \tag{33}$$
$$\kappa = \tfrac{1}{36}(-12\mu) \tag{34}$$
$$\eta = \tfrac{1}{36}(14 + 6\mu) \tag{35}$$
$$\xi = \tfrac{1}{36}(-2 + 6\mu) - \nu \tag{36}$$
$$\delta = \tfrac{1}{36}(-2 - 6\mu) - \epsilon \tag{37}$$
$$\gamma = \tfrac{1}{36}(4) + \epsilon + \nu \tag{38}$$
$$\beta = \tfrac{1}{36}(12 - 24\mu) - \epsilon \tag{39}$$
$$\alpha = \tfrac{1}{36}(24 + 24\mu) - \nu \tag{40}$$

Again, we can decompose the interpolating scheme's mask into convolution of a smaller mask with the mask of the three-direction box-spline (Figure 6). The values in the mask are:

$$\pi = \tfrac{1}{36}(-1 + 3\mu) - \nu \tag{41}$$

$$\begin{bmatrix} & & & \nu & \theta & \xi & \xi & \theta & \nu & & \\ & & \theta & \epsilon & \delta & \kappa & \delta & \epsilon & \theta & & \\ & \xi & \delta & 0 & \gamma & \gamma & 0 & \delta & \xi & & \\ \xi & \kappa & \gamma & \beta & \eta & \beta & \gamma & \kappa & \xi & & \\ \theta & \delta & \gamma & \eta & \alpha & \alpha & \eta & \gamma & \delta & \theta & \\ \nu & \epsilon & 0 & \beta & \alpha & 1 & \alpha & \beta & 0 & \epsilon & \nu \\ & \theta & \delta & \gamma & \eta & \alpha & \alpha & \eta & \gamma & \delta & \theta \\ & & \xi & \kappa & \gamma & \beta & \eta & \beta & \gamma & \kappa & \xi \\ & & & \xi & \delta & 0 & \gamma & \gamma & 0 & \delta & \xi \\ & & & & \theta & \epsilon & \delta & \kappa & \delta & \epsilon & \theta \\ & & & & & \nu & \theta & \xi & \xi & \theta & \nu \end{bmatrix} = \begin{bmatrix} 1 & 1 & 1 & & \\ 1 & 2 & 2 & 1 & \\ 1 & 2 & 3 & 2 & 1 \\ & 1 & 2 & 2 & 1 \\ & & 1 & 1 & 1 \end{bmatrix} * \begin{bmatrix} \nu & \pi & \pi & \nu & & & \\ \pi & \rho & \sigma & \rho & \pi & & \\ \pi & \sigma & \tau & \tau & \sigma & \pi & \\ \nu & \rho & \tau & \upsilon & \tau & \rho & \nu \\ & \pi & \sigma & \tau & \tau & \sigma & \pi \\ & & \pi & \rho & \sigma & \rho & \pi \\ & & & \nu & \pi & \pi & \nu \end{bmatrix}$$

Figure 6: The mask of the ternary interpolating scheme (left) can be decomposed into a discrete convolution of the three-direction box-spline mask (centre) with the mask at right.

$$\frac{1}{3^5}\begin{bmatrix} 1 & 1 & 1 & & \\ 1 & 2 & 2 & 1 & \\ 1 & 2 & 3 & 2 & 1 \\ & 1 & 2 & 2 & 1 \\ & & 1 & 1 & 1 \end{bmatrix} * \begin{bmatrix} 1 & 1 & 1 & & \\ 1 & 2 & 2 & 1 & \\ 1 & 2 & 3 & 2 & 1 \\ & 1 & 2 & 2 & 1 \\ & & 1 & 1 & 1 \end{bmatrix} * \begin{bmatrix} -2 & -2 & \\ -2 & 15 & -2 \\ & -2 & -2 \end{bmatrix}$$

Figure 7: For $\mu = \frac{1}{27}$, $\epsilon = \frac{-5}{243}$, and $\nu = \frac{-2}{243}$, the mask of the ternary interpolating scheme can be decomposed into a discrete convolution of the three-direction box-spline mask with itself and then with the small mask at right.

$$\rho = \tfrac{1}{36}(2 - 6\mu) + \epsilon \quad (42)$$
$$\sigma = \tfrac{1}{36}(-12\mu) - 2\epsilon + 2\nu \quad (43)$$
$$\tau = \tfrac{1}{36}(2 + 18\mu) + 2\epsilon - \nu \quad (44)$$
$$\upsilon = \tfrac{1}{36}(-36\mu) - 6\epsilon \quad (45)$$

We assume that this decomposition will allow us to follow Dyn's method for analysing convergence and smoothness using Laurent polynomials [1]. Again, it is not clear what other conclusions can be draw from this decomposition into a box-spline and a smaller mask, although we note that it allows for an implementation of the ternary scheme as a two-pass method.

For the special case of $\mu = \frac{1}{27}$, $\epsilon = \frac{-5}{243}$, and $\nu = \frac{-2}{243}$, the mask can be decomposed into the convolution of the three-direction box-spline with itself and then with a very small third mask. These masks are shown in Figure 7. Unfortunately, this setting of the parameters leads to a scheme which eigenanalysis shows is at most $C1$.

5 Basic eigenanalysis

Eigenanalysis provides various conditions on the continuity of the limit surface [7]. In particular, studying the eigenvalues provides necessary conditions, giving the *maximum* continuity which a scheme could exhibit. We demonstrate ranges of the three parameters for which the scheme *could* be $C2$. We show that, given certain conditions on the three parameters, the eigenvectors are such that the scheme has quadratic precision.

The region around a vertex mark point is shown in Figure 8. If

$$P^n = [A, B_1, B_2, B_3, B_4, B_5, B_6, C_1, C_2, C_3, C_4, C_5, C_6, D_1, D_2, D_3, D_4, D_5, D_6]^T$$

and

$$P^{n+1} = [a, b_1, b_2, b_3, b_4, b_5, b_6, c_1, c_2, c_3, c_4, c_5, c_6, d_1, d_2, d_3, d_4, d_5, d_6]^T$$

then

$$P^{n+1} = MP^n \tag{46}$$

where M is given in Figure 9. The eigenvalues of this matrix are:

$$\begin{array}{rl}
1 & \\
\frac{1}{3} & \text{(twice)} \\
\frac{1}{9} & \text{(three times)} \\
\frac{1}{6} - \frac{5}{6}\mu & \text{(three times)} \\
\frac{1}{9} - \frac{1}{3}\mu + 2\nu + \epsilon & \\
\frac{1}{12} - \frac{1}{4}\mu + \nu + \epsilon & \text{(twice)} \\
\frac{1}{18} - \frac{1}{2}\mu & \text{(three times)} \\
\frac{1}{36} - \frac{1}{12}\mu & \text{(twice)} \\
-\frac{1}{2}\mu - \nu - \frac{5}{2}\epsilon \pm \frac{1}{6}\sqrt{441\epsilon^2 + 126\mu\epsilon + 180\nu\epsilon + 9\mu^2 + 72\nu\mu - 180\nu^2 + 12\nu} &
\end{array}$$

Note that the last entry in this list represents two eigenvalues (the "±" on the square root) and that either of these two could be one of the larger eigenvalues, depending on the values of the parameters.

The eigenvectors associated with the first six eigenvalues in the list (1, $\frac{1}{3}$, $\frac{1}{3}$, $\frac{1}{9}$, $\frac{1}{9}$, $\frac{1}{9}$) are such that the scheme will have quadratic precision *if* these six eigenvalues are the six largest.

Analysing these eigenvalues for general μ, ν and ϵ could be tricky. Consider, however, the case $\nu = 0$ and $\epsilon = 0$. We get the eigenvalues:

$$\begin{array}{l}
1, \frac{1}{3}, \frac{1}{3}, \frac{1}{9}, \frac{1}{9}, \frac{1}{9}, -\mu, \frac{1}{6} - \frac{5}{6}\mu, \frac{1}{6} - \frac{5}{6}\mu, \frac{1}{6} - \frac{5}{6}\mu, \\
\frac{1}{9} - \frac{1}{3}\mu, \frac{1}{12} - \frac{1}{4}\mu, \frac{1}{12} - \frac{1}{4}\mu, \frac{1}{18} - \frac{1}{2}\mu, \frac{1}{18} - \frac{1}{2}\mu, \frac{1}{18} - \frac{1}{2}\mu, \frac{1}{36} - \frac{1}{12}\mu, \frac{1}{36} - \frac{1}{12}\mu, 0
\end{array}$$

which indicates that the limit surface could be $C2$ only for the range $\frac{1}{15} < \mu < \frac{1}{9}$. This is, unsurprisingly, the same range of values of μ as in the univariate case [5]. The first six eigenvalues are the same for all values of μ in this range. For the special value of $\mu = \frac{1}{11}$, the seventh eigenvalue is minimized and, indeed, the seventh through tenth eigenvalues are then all equal to $\frac{1}{11}$.

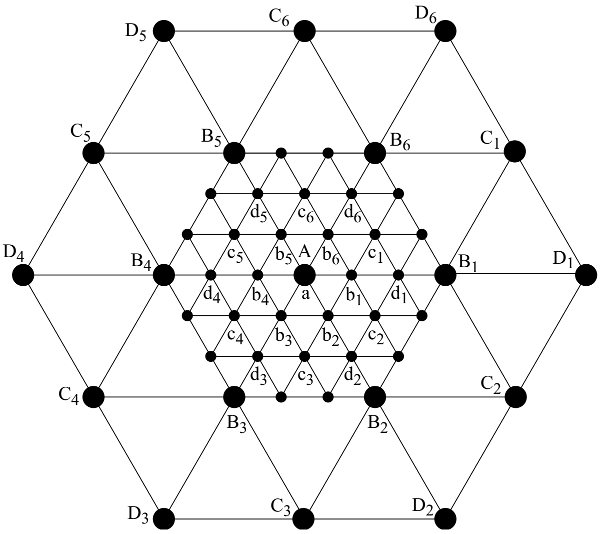

Figure 8: The region around a vertex mark point.

$$\left[\begin{array}{c|cccccc|cccccc|cccccc}
1 & 0 & 0 & 0 & 0 & 0 & 0 & 0 & 0 & 0 & 0 & 0 & 0 & 0 & 0 & 0 & 0 & 0 & 0 \\
\hline
\alpha & \beta & \gamma & \delta & \epsilon & \delta & \gamma & \xi & \xi & 0 & 0 & 0 & 0 & \nu & 0 & 0 & 0 & 0 & 0 \\
\alpha & \gamma & \beta & \gamma & \delta & \epsilon & \delta & 0 & \xi & \xi & 0 & 0 & 0 & 0 & \nu & 0 & 0 & 0 & 0 \\
\alpha & \delta & \gamma & \beta & \gamma & \delta & \epsilon & 0 & 0 & \xi & \xi & 0 & 0 & 0 & 0 & \nu & 0 & 0 & 0 \\
\alpha & \epsilon & \delta & \gamma & \beta & \gamma & \delta & 0 & 0 & 0 & \xi & \xi & 0 & 0 & 0 & 0 & \nu & 0 & 0 \\
\alpha & \delta & \epsilon & \delta & \gamma & \beta & \gamma & 0 & 0 & 0 & 0 & \xi & \xi & 0 & 0 & 0 & 0 & \nu & 0 \\
\alpha & \gamma & \delta & \epsilon & \delta & \gamma & \beta & \xi & 0 & 0 & 0 & 0 & \xi & 0 & 0 & 0 & 0 & 0 & \nu \\
\hline
\eta & \eta & \kappa & \theta & \theta & \kappa & \eta & \kappa & \theta & 0 & 0 & 0 & \theta & \theta & 0 & 0 & 0 & 0 & \theta \\
\eta & \eta & \eta & \kappa & \theta & \theta & \kappa & \theta & \kappa & \theta & 0 & 0 & 0 & \theta & \theta & 0 & 0 & 0 & 0 \\
\eta & \kappa & \eta & \eta & \kappa & \theta & \theta & 0 & \theta & \kappa & \theta & 0 & 0 & 0 & \theta & \theta & 0 & 0 & 0 \\
\eta & \theta & \kappa & \eta & \eta & \kappa & \theta & 0 & 0 & \theta & \kappa & \theta & 0 & 0 & 0 & \theta & \theta & 0 & 0 \\
\eta & \theta & \theta & \kappa & \eta & \eta & \kappa & 0 & 0 & 0 & \theta & \kappa & \theta & 0 & 0 & 0 & \theta & \theta & 0 \\
\eta & \kappa & \theta & \theta & \kappa & \eta & \eta & \theta & 0 & 0 & 0 & \theta & \kappa & 0 & 0 & 0 & 0 & \theta & \theta \\
\hline
\beta & \alpha & \gamma & \xi & \nu & \xi & \gamma & \delta & \delta & 0 & 0 & 0 & 0 & \epsilon & 0 & 0 & 0 & 0 & 0 \\
\beta & \gamma & \alpha & \gamma & \xi & \nu & \xi & 0 & \delta & \delta & 0 & 0 & 0 & 0 & \epsilon & 0 & 0 & 0 & 0 \\
\beta & \xi & \gamma & \alpha & \gamma & \xi & \nu & 0 & 0 & \delta & \delta & 0 & 0 & 0 & 0 & \epsilon & 0 & 0 & 0 \\
\beta & \nu & \xi & \gamma & \alpha & \gamma & \xi & 0 & 0 & 0 & \delta & \delta & 0 & 0 & 0 & 0 & \epsilon & 0 & 0 \\
\beta & \xi & \nu & \xi & \gamma & \alpha & \gamma & 0 & 0 & 0 & 0 & \delta & \delta & 0 & 0 & 0 & 0 & \epsilon & 0 \\
\beta & \gamma & \xi & \nu & \xi & \gamma & \alpha & \delta & 0 & 0 & 0 & 0 & \delta & 0 & 0 & 0 & 0 & 0 & \epsilon
\end{array}\right]$$

Figure 9: The matrix, M, around a vertex mark point. The horizontal and vertical lines are merely to show the internal structure of the matrix.

Consider now the behaviour of the other two free parameters. If we set $\mu = \frac{1}{11}$ and $\nu = 0$ while allowing ϵ to be free, we find the eigenvalues:

$$\begin{array}{l} 1, \frac{1}{3}, \frac{1}{3}, \frac{1}{9}, \frac{1}{9}, \frac{1}{9}, \frac{1}{11}, \frac{1}{11}, \frac{1}{11}, \frac{1}{99}, \frac{1}{99}, \frac{1}{99}, \\ -6\epsilon - \frac{1}{11}, \epsilon + \frac{8}{99}, \epsilon, \epsilon + \frac{2}{33}, \epsilon + \frac{2}{99}, \epsilon + \frac{2}{33}, \epsilon + \frac{2}{99}. \end{array}$$

This requires:

$$\frac{-10}{297} < \epsilon < \frac{1}{297}$$

as the maximum range for which the scheme could have $C2$ continuity with $\mu = \frac{1}{11}$ and $\nu = 0$.

Now, we do the same thing for ν, by setting $\mu = \frac{1}{11}$ and $\epsilon = 0$ while allowing ν to be free. We find the eigenvalues:

$$\begin{array}{l} 1, \frac{1}{3}, \frac{1}{3}, \frac{1}{9}, \frac{1}{9}, \frac{1}{9}, \frac{1}{11}, \frac{1}{11}, \frac{1}{11}, \frac{1}{99}, \frac{1}{99}, \frac{1}{99}, \\ -\nu - \frac{1}{22} \pm \frac{1}{66}\sqrt{-21780\nu^2 + 2244\nu + 9}, \\ 2\nu + \frac{8}{99}, \nu + \frac{2}{33}, \nu + \frac{2}{33}, -\nu + \frac{2}{99}, -\nu + \frac{2}{99}. \end{array}$$

Note that the expression containing the square root represents two different eigenvalues. The maximum range of values for which the scheme could be $C2$ is:

$$-0.003865 < \nu < 0.003587$$

to four significant digits, with $\mu = \frac{1}{11}$ and $\epsilon = 0$.

The special case shown in Figure 7 has, as its first nine eigenvalues:

$$1, \frac{1}{3}, \frac{1}{3}, \frac{11}{81}, \frac{11}{81}, \frac{11}{81}, \frac{1}{9}, \frac{1}{9}, \frac{1}{9}$$

which indicates that it is at most $C1$.

It is clear that ϵ and ν cannot vary far from zero and still retain the possibility that the limit surface is $C2$. There is, however, no clear intuition as to the effect on the limit surface of varying these parameters. It may be thought that $\nu = \epsilon = 0$ would be the best choice, but we note that this would create a scheme with fractal support [6]. Further analysis is required.

6 What we have proven so far

We have derived a ternary interpolating scheme for the regular triangular mesh. The scheme has three parameters: μ, ν, and ϵ. The scheme is $C2$ along each of the three principal directions of the mesh for $\frac{1}{15} < \mu < \frac{1}{9}$ for the case of data extruded along a principal direction. Eigenanalysis shows that for $\nu = 0$, and $\epsilon = 0$, the scheme could be $C2$ in the regular case for the same range of μ. Ranges for ν and ϵ have been found which retain this $C2$ condition for the case where the other parameter is set to zero and $\mu = \frac{1}{11}$. For values of μ, ν and ϵ for which the six largest eigenvalues are 1, $\frac{1}{3}$, $\frac{1}{3}$, $\frac{1}{9}$, $\frac{1}{9}$, $\frac{1}{9}$, the scheme has quadratic precision.

7 Remaining work

Several things are left to do.

- We need to perform continuity analysis on the scheme to ascertain the actual continuity of the limit surface in the regular case. More detailed eigenanalysis and Laurent polynomial (z-transform) analysis are thus required.
- We need to get some intuition as to the meaning of the new parameters, ν and ϵ, and find appropriate values for them.
- We need to work out what to do around extraordinary points.
- While every effort has been made to ensure the correctness of the derivation presented here, it would be helpful if the derivation of the ternary interpolating scheme's mask was independently checked for correctness.

Acknowledgements

This work has been supported by the European Union, under the ægis of the MINGLE project (HPRN–CT–1999–00117).

References

[1] N. Dyn. Analysis of convergence and smoothness by the formalism of Laurent polynomials. In A. Iske, E. Quak, and M.S. Floater, editors, *Tutorials on Multiresolution in Geometric Modelling*, chapter 3, pages 51–68. Springer, 2002.

[2] N. Dyn. Interpolatory subdivision schemes. In A. Iske, E. Quak, and M.S. Floater, editors, *Tutorials on Multiresolution in Geometric Modelling*, chapter 2, pages 25–50. Springer, 2002.

[3] N. Dyn, D. Levin, and J. A. Gregory. A butterfly subdivision scheme for surface interpolation with tension control. *ACM Transactions on Graphics*, 9(2):160–169, 1990.

[4] N. Dyn, D. Levin, and J.A. Gregory. A 4-point interpolatory subdivision scheme for curve design. *Computer Aided Geometric Design*, 4:257–268, 1987.

[5] M. F. Hassan, I. P. Ivrissimitzis, N. A. Dodgson, and M. A. Sabin. An interpolating 4-point C^2 ternary stationary subdivision scheme. *Computer Aided Geometric Design*, 19(1):1–18, January 2002.

[6] I. P. Ivrissimitzis, M. A. Sabin, and N. A. Dodgson. On the support of recursive subdivsion. submitted to *ACM Transactions on Graphics*.

[7] M. A. Sabin. Eigenanalysis and artifacts of subdivision curves and surfaces. In A. Iske, E. Quak, and M.S. Floater, editors, *Tutorials on Multiresolution in Geometric Modelling*, chapter 4, pages 69–92. Springer, 2002.